

Is the recently discovered large scale filamentary feature *Cattail* in the cold or unstable phase?

Ka Ho Yuen,^{1*} Avi Chen,² Ka Wai Ho,¹ Alex Lazarian^{1,3}

¹Department of Astronomy, University of Wisconsin-Madison, USA

²Department of Physics, City College, CUNY, USA

³Centro de Investigación en Astronomía, Universidad Bernardo O'Higgins, Santiago, General Gana 1760, 8370993, Chile

Accepted XXX. Received YYY; in original form ZZZ

ABSTRACT

A recent publication (Li et al. 2021) discovered one of the largest filamentary neutral hydrogen features dubbed *Cattail* from high resolution FAST observations that might be a new galactic arm of our own Milky Way. However in the analysis, it was suggested that this neutral hydrogen feature is cold despite having 12 km/s total linewidth. We evaluate the probability whether the *Cattail* is actually cold neutral media via the newly developed Velocity Decomposition Algorithm (Yuen et al. 2021a) and Force Balancing Model (Ho et al. 2021a). We discovered that even with the inclusion of the galactic shear term, the feature is still at the unstable neutral media regime. Moreover, we also discover that the *Cattail* is two disjoint features in caustics space, suggesting that the *Cattail* might have two different turbulent systems. We check the spectra of the individual system separated via VDA to confirm this argument. We do not exclude the existence of smaller scale cold media being embedded within this structure.

1 INTRODUCTION

The atomic hydrogen cold neutral media (HI-CNM) is one of the most important astrophysical observables. Observations like HI4PI Kalberla & Haud (2015), GALFA (Peek et al. 2018), THOR-HI (Beuther et al. 2016; Wang et al. 2020), FAST (Li et al. 2021) have improved our understanding of CNM, including its relation to the underlying molecular phase Kritsuk et al. (2017), correlation to magnetic fields (Heiles, C 2001; Clark et al. 2015), and its spatial distribution (Kalberla et al. 2016; Kalberla & Haud 2018). CNM is ubiquitous in the interstellar media (ISM) for both high latitude (Clark et al. 2014, 2015) and galactic plane (Soler et al. 2020). The linear features of CNM makes it one of the most important B-field probes in modern astronomy, with vast applications from cosmology (Clark & Hensley (2019)) to diffuse molecular cloud studies (e.g., Clark et al. 2014; Lazarian et al. 2018).

Recently a large, cold HI filamentary feature was discovered by Li et al. (2021) and was dubbed "Cattail". The feature is thought to be either a new galactic arm, or the furthest and largest cold gas filament in our galaxy. It is located near the galactic plane. Its length is either 1.1 kpc or as large as 5 kpc¹ and its width is 200 pc. It is located 22 kpc away from the galactic center, in the Extreme Outer Galaxy (EOG) with a 5:1 aspect ratio. It was observed using

Five-hundred-meter Aperture Spherical radio Telescope (FAST) on August 24 2019.

Cattail is believed to be cold.² It is, however, relatively diffuse (0.03 cm^{-3}) and possesses a relatively large linewidth (12 km/s). These characteristics are uncommon for CNM. A typical cold filament at $M_s = 3$ and $T = 200\text{ K}$ has a thermal linewidth of $v = 4 - 6\text{ km/s}$ along the line of sight (Kalberla & Haud 2018). Li et al. (2021) associates the large linewidth with the galactic rotation.³ However, even taking the upper estimate of the galactic rotation curve (see Mrož 2019), at 22 kpc, its contribution is roughly $300\text{ km/s} \times (200\text{ pc})/22\text{ kpc} \sim 2.7\text{ km/s}$. Combining the turbulent and thermal linewidth there is roughly 4-6 km/s of linewidth discrepancy, if we simply assume the *Cattail*'s linewidth is from turbulence, CNM thermal broadening and galactic rotation alone. The 12 km/s linewidth that is seen in *Cattail* is, therefore, not consistent with the suggestion that it is CNM.

In this paper we will take a step back and reanalyse the *Cattail* region using the statistics of turbulence via the Velocity Decomposition Algorithm (VDA) and a recently theorized Force Balancing Model Ho et al. (2021a). We shall show that the *Cattail* is not a cold but a transient unstable neutral media (UNM) with significant contributions of turbulence. We will also show that it is likely not a statistically coherent 5 kpc long region. In §2 we briefly discuss why VDA is important in classifying CNM and UNM, and the major findings of VDA and Force Balancing Model. In §3 we discuss our results. In §4 we argue quantitatively why *Cattail* is likely not cold.

¹ Li et al. (2021) is not clear on the definition of *Cattail*. In the introduction it is stated that *Cattail* is 1.1 kpc or as large as 5 kpc. Their table 1, which lists the properties of *Cattail* including its 1.1 kpc length refers only to the FAST observation at the tip of *Cattail*, i.e. a "small" clump with length 1.1 kpc and width 200 pc. However, starting from page 5, *Cattail* is defined as the giant filament with length 5 kpc, and the paper concludes that "we suggest two possible explanations for *Cattail*: it is a giant filament with a length of 5 kpc, or part of a new arm in the EOG [Extreme Outer Galaxy]". In this paper, due to the limitation of the resolution from HI4PI, we focus on the entire filament. Notice that the tip of *Cattail* has higher density, so we expect the entire filament to have lower density on average.

² Li et al "HI filaments are normally cold with typical excitation temperature (50K), corresponding to an isothermal sound speed of approximately 0.65 km/s. Therefore, the turbulence may be supersonic in *Cattail*."

³ "... there is no evidence for *Cattail*'s velocity coming from the influences of stellar feedback or a tidal stream, the most likely explanation is the Galactic Rotation."

In §5 we discuss the importance of *Cattail* being UNM, and in §6 we conclude our paper.

2 APPLYING THE FINDINGS OF VDA TO CATTAIL

In Yuen et al. (2021a) a novel technique was presented to reconstruct the velocity caustics p_v ⁴ from each channel based on a linear algebra formalism. The technique, among other things, applied the theoretical results established by Lazarian & Pogosyan (2000, 2004). The formalism is known to work in multiphase HI media, and tested both in numerics and observations in Yuen et al. (2021a). To summarize, the density fluctuation p_d and velocity caustics p_v (which together make up velocity channels in PPV cubes) can be obtained from the following formulae with the full PPV cube $p(\mathbf{R}, v)$ and the column intensity map $I(\mathbf{R})$:

$$p_v = p - (\langle pI \rangle - \langle p \rangle \langle I \rangle) \frac{I - \langle I \rangle}{\sigma_I^2}$$

$$p_d = p - p_v \quad (1)$$

$$p_d = (\langle pI \rangle - \langle p \rangle \langle I \rangle) \frac{I - \langle I \rangle}{\sigma_I^2}$$

The VDA can determine the relative density-to-velocity fluctuations in HI velocity channel maps. This is illustrated with the $\sigma - v$ and P_d/P_v diagrams. The $\sigma - v$ diagram measures the dispersions of p_d and p_v as a function of line-of-sight velocity and tells us whether a particular channel is velocity or density dominant. The P_d/P_v diagram measures the relative importance of density and velocity fluctuations as a function of spatial scales on the plane of sky and also tells us whether a particular channel is velocity or density dominant in different length scales.

The VDA uses the velocity and density contributions in channel maps to determine whether turbulence is dominant over the thermal contributions. If channel maps are velocity dominant (i.e. $P_d/P_v < 1$) then turbulence is dominant and it will have larger contribution to the linewidth. VDA also allows us to evaluate the importance of turbulence via the visual feature in the caustics map: The more turbulent the system, the more fractured the caustic map.

VDA can distinguish whether the feature is subjected to strong thermal broadening. Yuen et al. (2021a) show that in the presence of strong thermal broadening, the channel maps across the linewidth would visually look the same. However, CNM is supersonic in nature and has weak thermal broadening. Thus, when we are examining velocity channels whose width is thinner than the turbulent linewidth, the CNM features will look different in different channels, while the strongly thermal broadened features (UNM, WNM) will look the same across the channels. The VDA, therefore, allows us to distinguish whether the visual features in the channel maps are cold or not.

Recently Ho et al. (2021a) proposed a Force Balancing Model that predicts the aspect ratio of the CNM by considering the force balances between the UNM and CNM. Their result showed that the aspect ratio of *dynamically stable* CNM in typical turbulence

⁴ Velocity caustics represent the velocity contributions to channel maps. Caustics are generally caused by critical points of the phase in differential maps thereby creating a hyper-surface in the space of parameters (See Arnold et al. (1985)). They cause a diverging intensity in the PPV cube which show up as elongated regions in channel maps. These features do not correspond to any physical density.

($M_s \approx 3$, $M_A \approx 0.5$) and density conditions for far-away arms ($n_{CNM, 18kpc} \approx 1 cm^{-3}$, $n_{UNM, 18kpc} \approx 0.1 cm^{-3}$, Wolfire et al. 2003) should be at the order of unity, which is significantly smaller than the currently circulating estimate using the Goldreich & Sridhar scaling, (1995, see, e.g. Xu et al. (2019)). Notice that if the observed CNM is longer than the theoretical estimate from Ho et al. (2021a), it is dynamically unstable and will soon fragment into shorter clumps. Ho et al. (2021a) suggests a new type of instability generated from an attractive pressure force from the UNM. WNM are subjected to Goldreich & Sridhar turbulence since critical balance holds in WNM. However, during the formation of CNM, the pressure balance between the UNM attractive pressure force and the CNM repulsive pressure force along the perpendicular direction of the magnetic field will restrict the length and width of the newly formed CNM. From Ho et al. (2021a):

$$\text{Aspect ratio} \approx \frac{M_s^2}{M_A} [25.6 \frac{l_{\perp}}{l_{U,\perp}} - 2(\frac{n_{peak}}{n_C} - 1)]^{-1} \quad (2)$$

where $M_{s,A}$ are the sonic and Alfvénic Mach numbers, l_{\perp} is the perpendicular CNM width, $l_{U,\perp}$ is the perpendicular UNM width, n_{peak} is the peak number density for CNM which is restricted by the HI-H2 conversion, and n_C is the mean density of the CNM. Notice that Eq.2 is useful in quantifying whether a particular feature is a dynamically stable CNM.

VDA can also determine whether the structures in channel maps are part of the same turbulent system. In Yuen et al. (2021b), it is shown that: (1) features that are magnetized and parallel to the magnetic fields tend to have a density spectral power slope of -2 ; (2) if the feature is not magnetized, the density power spectral slope is steeper and can be as most as $-11/3 \approx -3.7$ (See e.g. Lazarian & Pogosyan (2000, 2004)). By examining the power spectra of each individual regions in the *Cattail*, we can determine whether the structures are likely in the same turbulence system. VDA also demonstrates that when features are disjoint in the caustic map they are unlikely to be a part of the same turbulent system (See also ?population).

3 RESULTS

To show that the *Cattail* (1.1 kpc region) is likely not in the CNM (and therefore likely to be UNM), we establish that: (1) There is a significant turbulent velocity fluctuation in the *Cattail* region (2) the region is thermally dominant (3) It is not dynamically stable if it is CNM Ho et al. (2021a).

3.1 VDA reveals the existence of Kolmogorov turbulence cascade in *Cattail*

Since *Cattail* is at the edge of the spectral line, using the $\sigma - v$ diagram in analyzing the relative fluctuations across v requires additional consideration (Yuen et. al in prep). Hence we can only use the P_d/P_v diagram. The left of Fig.3 shows the spectrum ratio of the density and velocity fluctuations P_d/P_v in the "grand" (i.e. 5kpc) *Cattail* region for the 4 selected thin⁵ velocity slices as shown in Fig.1. We can see from this figure that the intermediate and small scale fluctuations in channel maps do indeed correspond to the velocity fluctuations since $P_d/P_v \ll 1$ roughly at 0.3 – 2.0 kpc. This indicates a strong turbulent imprint in the *Cattail* region over a range of velocity slices,

⁵ Lazarian & Pogosyan (2000) defines "thin" velocity channel when the channel width Δv is smaller than the spatial velocity dispersion $\delta v(R)$.

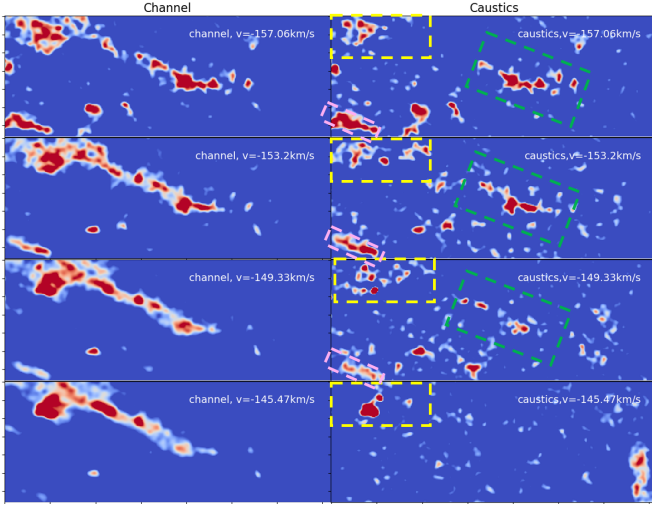


Figure 1. A set of figures showing the fluctuations of velocity channels (left) and caustics (right) at least $0.8\sigma - 3\sigma$ above the mean value for different selected velocities. Here we marked three spatially separate regions for our discussions in §3.4. The green region correspond to the tip of the *Cattail* (the 1.1 kpc one) that is discussed in the first half of (Li et al. 2021).

especially for the smaller *Cattail* region (1.1 kpc). To show that this region is also velocity dominant, on the right of the Fig. 3 we perform the same P_d/P_v analysis by focusing only on the green box. Notice that the velocity fluctuation at $v = -145$ is almost zero visually (See the lower right panel of Fig. 1), therefore this line is excluded. We can see from the right of Fig. 3 that the entire "smaller" *Cattail* region is velocity dominant, meaning turbulence contributes significantly to the linewidth. This contribution is roughly $3 - 5 \text{ km/s}$ (Kalberla et al. 2016)⁶.

In theory one can determine the strength of the thermal broadening by inspecting the channel map, however showing that the thermal broadening exist does not mean that turbulence fluctuations exist in channel maps (See, counterexamples from Clark et al. 2019 and also Yuen et al. 2019). Our result in this subsection shows that the turbulence fluctuations indeed exist and follows the expected Kolmogorov cascade (See also Yuen et al. (2021b)).

3.2 VDA confirms the strong thermal broadening signal

We apply Eq.1 and visually inspect the fluctuations of thin channels near the *Cattail* region (in this instance the channels are thin because $\Delta v \sim 1.288 \text{ km/s}$ (the slices in PPV) $< v_{turb}$ ($3 - 5 \text{ km/s}$) (see Lazarian & Pogosyan (2000, 2004); Lazarian & Yuen (2018) for a precise definition of thin channels) near the *Cattail* region. If the feature is not subject to strong thermal broadening we expect to see a change of channel map features over neighboring channels due to caustics fluctuations. Fig.1 shows the fluctuations of HI channel map and caustics map side by side via VDA with fluctuations above mean for at least

⁶ The $3 - 5 \text{ km/s}$ contribution of turbulence to the linewidth is just a rough estimate. It is a well-known that turbulence linewidth does not significantly vary in multiphase media (Kritsuk et al. (2017)). The lower estimate of 3 km/s comes from Kalberla et al. (2016) by the full width half maximum of the decomposed CNM. While the 5 km/s estimate came from Kalberla & Haud (2018) where the authors are fitting the CNM multi-Gaussian spectral line. This estimate has also been verified numerically. See Appendix

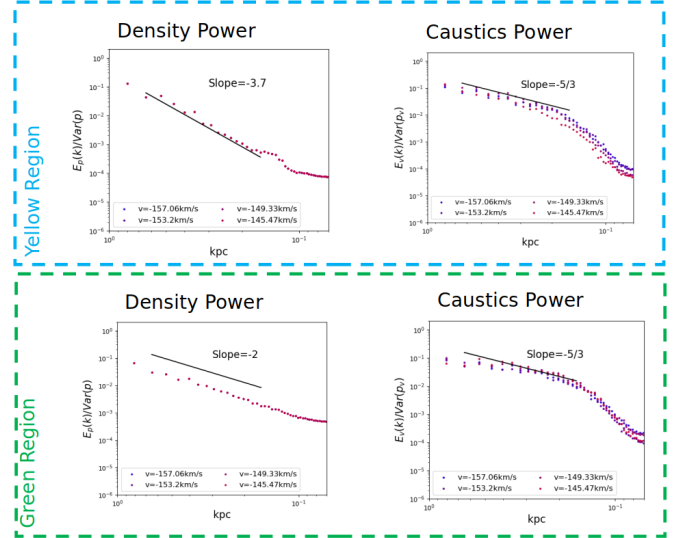


Figure 2. Four figures showing the variation of the normalized power spectra for the 4 selected velocity slices as a function of length scales (in kpc). From top left: p_d for the yellow region; top right: p_v for yellow region; lower left: p_d for the green region; lower right: p_v for the green region.

0.8σ . This guarantees the noise contribution will be eliminated. According to VDA, only when the system is thermally dominant will the channel maps look more or less the same across different velocities. In this scenario, VDA will remove the contributions due to thermal broadening and reveal the real turbulent fluctuations of the system in the caustic map. We can easily recognize that the *Cattail* features in channel maps stay pretty much the same over 10 km/s, thus indicating the presence of strong thermal broadening.

3.3 Force Balancing Model shows that *Cattail* is dynamically unstable if CNM

To proceed with applying the Force Balancing Model to *Cattail* we have to estimate the parameters in Eq.2 using :

M_S : Using our estimation on the thermal linewidth from §3.4, we see that $M_S \approx \sqrt{3}v_{turb}/c_s \approx 1$.

M_A : We can utilize a simple scaling relation to approximate the M_A at 22 kpc using the M_A estimates of ~ 0.5 from nearby CNM (Yuen & Lazarian 2020b): $M_A(R = 22 \text{ kpc}) \sim \sqrt{\frac{n_H(R=22 \text{ kpc})}{n_H(R=0 \text{ kpc})}} M_A(R = 0 \text{ kpc})$ (using n_H from Li et al. (2021)). Given that n_H in $R=0 \text{ kpc}$ is $\sim 10 \text{ cm}^{-3}$, M_A at 22 kpc is roughly $\sqrt{0.03/10} \times 0.5 \sim 0.02$, which agrees with the visual absence of the structure curvature in the *Cattail* region (Yuen & Lazarian 2020b).

$l_{\perp}/l_{U,\perp}$: The factor in the bracket depends on two parameters. The $l_{\perp}/l_{U,\perp}$ parameter can be approximated by the volume fraction of CNM and UNM similar to Ho et al. (2021a) as 1 (which corresponds to $CNM : UNM \sim 1 : 8$ in volume fractions).

n_{peak}/n_C : The other parameter n_{peak}/n_C can be estimated by the peak intensity value near the *Cattail* region ($1.7 \times 10^{19} \text{ cm}^{-2}$)

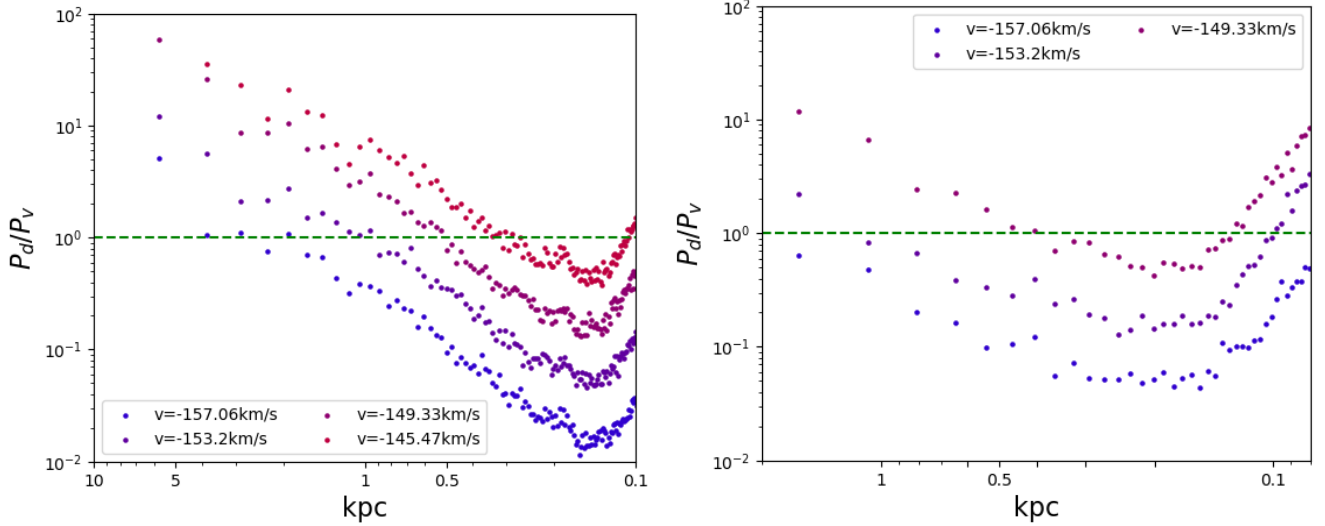


Figure 3. (Left) A figure showing the spectrum ratio of the density and velocity fluctuations P_d/P_v in the grand *Cattail* (5kpc) region for the 4 selected velocity slices as a function of length scales (in kpc) in Fig.1. (Right) The P_d/P_v analysis for the tip of the *Cattail* (1.1kpc) region. Notice that we exclude $v = -145\text{km/s}$ for this panel because there are no noticeable caustics contribution as we see in Fig. 1.

over their "CNM" mean volume density estimates (0.03cm^{-3}) times their estimated LOS distance (200pc) which is roughly 1.

Summarizing these numbers, we have an estimate for the aspect ratio that is not much deviated from unity. According to Ho et al. (2021a) this indicates that if *Cattail* is CNM, it is unlikely to be dynamically stable, i.e. it will be fragmented in the foreseeable future. In addition, in the whole *Cattail* (5 kpc) we observe a number of clumpy, circular features from visual inspections in velocity channels. These clumpy, spherical features are inconsistent with the usual expectation that the CNM is highly anisotropic and elongated along B-field.

3.4 VDA also shows that *Cattail* consists of multiple systems and likely does not extend for 5 kpc as a single turbulent system

From the visual inspection of Fig.1, we can see that near the mean velocity of *Cattail* ($v \sim 151\text{km/s}$), the fluctuations of velocity caustics are actually spatially separated into a few groups. We draw their boundaries with rectangular boxes. Notice that the green region is the "smaller" *Cattail* that is defined in the first half of Li et al. (2021) paper. These features seem to be connected in channel maps but are disjoint in all caustics maps. The disconnection of features are also seen if one inspects the velocity channels $v < -158\text{km/s}$. We also analyze the velocity caustics power spectrum for the yellow and green regions labelled in Fig.1. The left of Fig.2 shows the power spectra for both p_d and p_v in the green and yellow regions. We can see that the slope of their density power spectra are different: The green region has a density spectral slope of -2 , which indicates the feature is magnetized and parallel to the magnetic field (Yuen et al. 2021b; Ho et al. 2022), while in the yellow region we observe a density power spectral slope of ~ -3.7 , which is a signature of weakly magnetized turbulence. This difference suggests that the yellow and the green region are not in the same turbulent system. As a result it is very unlikely that *Cattail* can be considered as a coherent region 5 kpc long.

4 QUANTITATIVE ARGUMENT WHY THE TIP OF CATTAIL IS UNLIKELY COLD

By combining the facts in §3, we see that the *Cattail* is unlikely to be CNM. In this section we shall give quantitative arguments that is consistent with our results.

Discrepancy of linewidth contribution even with the presence of galactic rotation curve We discussed in the introduction that even considering the galactic rotation contributions, it is very unlikely that the *Cattail* at $T = 200\text{K}$ will have a linewidth of 12km/s , unless there are other physical processes occurring in *Cattail*, such as outflow velocities along the line of sight, supernova/shock driven bubbles etc. However, it is hard to imagine that these physical processes are happening at length scales of 1 kpc (or 5 kpc, depending on the definition of *Cattail*) at 22 kpc away from the galactic center given that the region seems to be self-isolated. It is therefore more natural to assume that the contributions of linewidth are only from turbulence, galactic shear and thermal broadening.

Shear galactic rotation at 22 kpc contributes roughly 3km/s to *Cattail's* linewidth.⁷ Turbulence also contributes roughly $3 - 5\text{km/s}$ to the linewidth (See §3.1). If there are no contributions from other physical processes, then the thermal width is estimated to be $4 - 6\text{km/s}$. This will corresponds to a temperature of 940K ($\bar{c}_s = 4\text{km/s}$) to 2130K ($\bar{c}_s = 6\text{km/s}$)⁸, consistent with the temperature range of the UNM⁹. However in §5 we emphasize that we cannot

⁷ In Li et al. (2021) the line of sight depth of *Cattail* is estimated to be 200pc . We choose the very upper estimate of a flat galactic rotation curve model of the Milky Way $v_{\text{rotation}} < 300\text{km/s}$. For a 200pc object, this will naturally introduce a total amount of **internal** shear of $300\text{km/s} \times 200\text{pc}/22\text{kpc} < 3\text{km/s}$. We also assume that the shear contribution is all projected along the line of sight. This would constitute the upper estimate of shear contribution. The choice of upper estimate is to minimize the thermal width estimated in this section to make it colder.

⁸ $T \sim (v/13\text{km/s})^2 \times 10,000\text{K}$

⁹ Noticing that the definition of CNM in terms of temperature changes as a function of the cooling and heating function. However CNM rarely will be at $T=1000\text{K}$, see Wolfire et al. 2003.

solely use the temperature to determine the phases. More importantly, we also do not exclude the possibility that the region might be a mixture of warm and cold gases as proposed by [Kalberla & Dedes \(2008\)](#).

Density too small to be CNM At the outer parts of the galaxy it is hard to achieve the tight pressure balances suggested by [Field et al. \(1969\)](#). Yet one can still assume that such a balance occurs and consider the properties of the unstable and cold phase with the density and the temperature quoted from [Li et al. \(2021\)](#). We find that these numbers can be roughly compared *order of magnitude wise* with the 18 kpc result from [Wolfire et al. \(2003\)](#). Although from [Kalberla & Kerp \(2009\)](#) we see that the mean density of the HI clouds at 22 kpc is of the order 0.01cm^{-3} , this density corresponds to the warm gases rather than the cold gases. The density of the CNM is at least 30-70 times that of WNM (e.g. compare Table 3 of [Wolfire et al. \(2003\)](#) to that of Fig 4 of [Kalberla & Kerp \(2009\)](#)). Therefore a rough estimation of the CNM density in *Cattail* should be $n_{\text{CNM}} \sim 50 \times n_{\text{Cattail}} \sim 1.5\text{cm}^{-3}$.

Pressure too small to be CNM It is also apparent that the pressure estimate from the numbers given by [Li et al. \(2021\)](#) is too low compared to [Wolfire et al. \(2003\)](#). By a simple computation, $P/k_B \sim 0.03 \times 200 \sim 6\text{Kcm}^{-3}$. Yet in [Wolfire et al. \(2003\)](#), the pressure at 18kpc is roughly $0.025 \times 8000 \sim 200\text{Kcm}^{-3}$. Assuming proper interpolations, the estimation of the pressure of *Cattail*, if it is CNM, is still two orders of magnitude lower than that of Fig 9 of [Wolfire et al. \(2003\)](#) and Fig 12 of [Kalberla & Kerp \(2009\)](#).

5 DISCUSSIONS

5.1 The Importance of understanding the UNM

The definition of CNM is not well defined despite being used for many years in the literature. Employing varying definitions (200-700K), the UNM regime (ranging from 200K to 600K, see also [Murray et al. \(2018\)](#)) is often miss-categorized as the "cold phase". This temperature-based classification of CNM often lead to erroneous conclusions in terms of its physical properties, e.g. an inadmissible aspect ratio for CNM [Ho et al. \(2021a\)](#). One should therefore take caution that any definition of CNM should be given by the respective phase diagram defined by the balances of heating and cooling rates as opposed to a specified temperature threshold.

The UNM plays a significant role in many interstellar processes. Having high mass and volume fraction (40% for both, [Kalberla et al. \(2016\)](#)), UNM controls the formation and shaping of CNM features (See [Ho et al. \(2021a\)](#)) by providing additional stability to the CNM at the cost of smaller aspect ratio. Due to strong self-absorption (when cold HI in the foreground absorbs the emission of warmer HI in the background) and quick H2 conversion lifetime [Bialy & Sternberg \(2016\)](#), it was recently suggested [Seifried et al. \(2021\)](#) that the HI emission map might actually not detecting all of the CNM. Moreover, UNM has generally longer aspect ratio than the embedded CNM [Ho et al. \(2021a\)](#), which is believed to be the result of the grand cascade despite [Goldreich & Sridhar](#) scaling not being relevant during the phase transition. Turbulence also plays an important role in maintaining the existence and stability of the UNM ([Ho et al. 2021b](#)). Indeed, if magnetized turbulence is not involved in the formation of UNM, the observed fraction of UNM will be significantly lower and UNM will quickly dissipate. Simulations ([Audit & Hennebelle 2005](#); [Kritsuk et al. 2017](#); [Ho et al. 2021a](#); [Murray et al. 2018](#); [Ho et al. 2021b](#)) showed that the UNM with

adequate turbulent injection will display a mass/volume fraction of 0.4, and is consistent with observational findings ([Kalberla & Haud \(2018\)](#) mass fraction \sim volume fraction \sim 0.4). Observing a huge, linear UNM on the sky (e.g. 1.1 kpc *Cattail*) would be a huge step in understanding the actual dynamics of UNM and how it impacts the formation of CNM especially with better interferometric instruments like FAST.

5.2 Kolmogorov cascade observationally verified in *Cattail*

In this paper, We showed that turbulence is an essential component in *Cattail*. In fact, from our analysis, we see that a grand Kolmogorov $-5/3$ cascade can be recovered via caustic maps, despite the channel maps not having such power scaling. It has been strongly postulated that turbulence cascades from very large scale down to cores and filaments, but the only observational proof aside from the Larson's classic paper (1981) is the electron density power spectra provided by [Chepurnov & Lazarian \(2010\)](#) and [Armstrong et al. \(1995\)](#). However, the most important and dynamical length scales, 0.01 pc to 10 kpc, where the entire dynamics of HI and some of H2, are not covered, and the evidence of Kolmogorov cascade is subject to outlier effect. [Yuen et al. \(2021b\)](#) recently showed a grand Kolmogorov $-5/3$ caustics cascade from >100 pc down to 0.01 pc using data from multiple tracers. Our study complements the study ([Yuen et al. 2021b](#)) that even at the length scale of *Cattail* (\sim kpc), we can still recover the Kolmogorov $-5/3$ slope from caustics power spectrum, indicating the relevance of Kolmogorov-type cascade (including [Goldreich & Sridhar \(1995\)](#)) in multiphase media.

5.3 A cold neutral media candidate discovered in VDA

From our analysis we observe a much smaller and compact region, which we labelled in Fig.1 in a pink rectangle, that is not removed by VDA. We recognize that this smaller region has a much smaller linewidth ($\langle v \rangle \sim 160\text{km/s}$, $\Delta v \sim 5\text{km/s}$), consistent with the linewidth estimation of the CNM in the nearby galactic arm. This smaller filament is anisotropic, and has a rough aspect ratio of 3-5 (which is plausible since the permitted aspect ratio is larger for stable CNM as aspect ratio $\propto M_s^2$), consistent with the [Ho et al. \(2021a\)](#) restriction on stable CNM aspect ratio.

6 CONCLUSION

In this paper, we analyze the *Cattail* with the VDA and Force Balancing Model. We provide a simple analysis to determine the turbulent, thermal and dynamical properties of the *Cattail* region.. We find that:

- (i) The *Cattail* is likely to be in UNM (§3, §4).
- (ii) The *Cattail* region is turbulent (§3.1, Fig 3)
- (iii) The clumpy feature in *Cattail* is explained by the instability happening due to the existence of UNM (§3.3)
- (iv) The *Cattail* consists of several turbulent system and likely does not extend 5 kpc as a single turbulent system (§3.4 Fig.1)
- (v) The caustics power spectra for different regions of *Cattail* exhibit the Kolmogorov $-5/3$ law, which is consistent with [Yuen et al. \(2021b\)](#) (§3.2,5.2 Fig.2)

The first finding of a massive UNM filament will likely help us to understand the properties of multiphase HI more clearly in the near future.

Acknowledgment K.H.Y., K.W.H. & A.L. acknowledge the support

the NSF AST 1816234, NASA TCAN 144AAG1967 and NASA ATP AAH7546. The numerical part of the research used resources of both Center for High Throughput Computing (CHTC) at the University of Wisconsin and National Energy Research Scientific Computing Center (NERSC), a U.S. Department of Energy Office of Science User Facility operated under Contract No. DE-AC02-05CH11231, as allocated by TCAN 144AAG1967. K.H.Y, K.W.H acknowledges Chi Yan Law (Chalmers) for discussions.

REFERENCES

- Armstrong, J. W., Rickett, B. J., & Spangler, S. R. 1995, *The Astrophysical Journal*, **443**, 209
- Arnold, V.I., Varchenko, A. and Gusein-Zade, S.M., Singularities of Differentiable Maps: Volume I: The Classification of Critical Points Caustics and Wave Fronts, 1985, Birkhauser, Boston
- Audit, E., & Hennebelle, P., 2005, *A&A*, **433**, 1
- Andr , P., 2017, arXiv:1710.01030
- Bialy S., Sternberg A., 2016, *ApJ*, **822**, 83. doi:10.3847/0004-637X/822/2/83
- Beuther H., Bihl S., Rugel M., Johnston K., Wang Y., Walter F., Brunthaler A., et al., 2016, *A&A*, **595**, A32. doi:10.1051/0004-6361/201629143
- Chepurnov, A., & Lazarian, A. 2010, *The Astrophysical Journal*, Volume **710**, Issue 1, pp. 853-858 (2010), **710**, 853
- Clark, S. E., Peek, J. E. G., & Putman, M. E. 2014, *ApJ*, **789**, 82
- Clark, S. E., Hill, J. C., Peek, J. E. G., Putman, M. E., & Babler, B. L. 2015, *Physical Review Letters*, **115**, 241302
- Clark, S. E., Peek, J. E. G., & Miville-Deschenes, M.-A. 2019, *ApJ*, **874**, 171
- Clark S. E., Hensley B. S., 2019, *ApJ*, **887**, 136. doi:10.3847/1538-4357/ab5803
- Crutcher R., Heiles C., Troland T. (2003) Observations of Interstellar Magnetic Fields. In: Falgarone E., Passot T. (eds) Turbulence and Magnetic Fields in Astrophysics. Lecture Notes in Physics, vol 614. Springer, Berlin, Heidelberg. https://doi.org/10.1007/3-540-36238-X_6
- Field, G. B., Goldsmith, D. W., Habing, H. J. 1969, *ApJ*, **155**, L149
- Goldreich, P., Sridhar, S. 1995, *The Astronomical Journal*, **438**, 763
- K. W. Ho, K. H. Yuen, Lazarian, A., 2021a, submitted to MNRAS
- K. W. Ho, K. H. Yuen, Lazarian, A., 2021b, submitted to MNRAS
- K. W. Ho, K. H. Yuen, Lazarian, A., in preparation
- Heiles, C., 2001, *ApJ*, **551**, 105
- Kalberla, P.M.W., & Dedes, L., 2008, *A&A* **487**, 951
- Kalberla, P. M. W., & Kerp, J. 2009, *ARA&A*, **47**, 27
- Kalberla, P. M. W., Kerp, J., Haud, U., et al. 2016, *ApJ*, **821**, 117
- Kalberla P. M. W., Haud U., 2015, *A&A*, **578**, A78. doi:10.1051/0004-6361/201525859
- Kalberla P. M. W., Haud U., 2018, *A&A*, **619**, A58. doi:10.1051/0004-6361/201833146
- Kalberla, P. M. W., & Haud, U. 2019, *A&A*, **627**, A112
- Kritsuk, A. G., Ustyugov, S. D., Norman, M. L. 2017 *New J. Phys.* **19** 065003
- Kandel, D., Lazarian, A., & Pogosyan, D. 2016, *MNRAS*, **461**, 1227
- Kandel, D., Lazarian, A., & Pogosyan, D. 2017, *MNRAS*, **464**, 3617
- Kandel, D., Lazarian, A., & Pogosyan, D. 2017, *MNRAS*, **470**, 3103
- Li, C., Qiu, K., Hu, B., et al., 2021, *ApJ*, **918**:L2
- Lazarian, A., & Pogosyan, D. 2000, *ApJ*, **537**, 720
- Lazarian, A., & Pogosyan, D. 2004, *ApJ*, **616**, 943
- Lazarian, A., Yuen, K. H., Lee, H., & Cho, J. 2017, *ApJ*, **842**, 30
- Lazarian, A., & Yuen, K. H. 2018, *ApJ*, **853**, 96
- Lazarian, A., Yuen, K. H., Ho, K. W., et al. 2018, *ApJ*, **865**, 46.
- Lazarian, A., Yuen, K. H., & Pogosyan, D. 2020, arXiv:2002.07996, submitted to *ApJ*
- Lazarian, A., Yuen, K. H., & Pogosyan, D. 2021, submitted to *ApJ*
- Murray, C. E., Stanimirovi , Goss, W. M. (2018) *ApJ* **238**, 14
- Mro , P., Udalski, A., Skowron, D. M., et al., (2019) *ApJ* **870**:L10
- McClure-Griffiths, N. M., Dickey, J. M., Gaensler, B. M., Green, A. J., & Haverkorn, M. 2006, *ApJ*, **652**, 1339
- Peek, J. E. G., Babler, B. L., Zheng, Y., et al. 2018, *ApJS*, **234**, 2
- Seifried, D., Beuther, H., Walch, S. (2021), arXiv:2109.10917

	Weak field case		
	n_0 = 3		
	B_0 = 1		
	WNM	UNM	CNM
M_S	0.7	1.6	6.0
M_A	0.8	1.6	2.2
Mass filling factor $M_{C/U/W}$	0.08	0.28	0.63
Volume filling factor $V_{C/U/W}$	0.61	0.31	0.070

Table A1. Simulation parameters and the basic statistics for each phase in our multiphase simulation, from (Yuen et al. 2021a; Ho et al. 2021a).

- Soler, J. D., Beuther, H., Syed, J., et al. (2020), *A&A*, **642**, A163
- Wang Y., Beuther H., Rugel M. R., Soler J. D., Stil J. M., Ott J., Bihl S., et al, 2020, *A&A*, **634**, A83. doi:10.1051/0004-6361/201937095
- Wolfire M. G., McKee C. F., Hollenbach D., Tielens A. G. G. M., 2003, *ApJ*, **587**, 278
- Xu, S., Ji, S., & Lazarian, A. 2019, *ApJ*, **878**, 157
- Yuen, K. H., & Lazarian, A. 2017, *ApJ*, **837**, L24
- Yuen, K. H., & Lazarian, A. 2017, arXiv:1703.03026
- Lazarian, A., & Yuen, K. H. 2018, *ApJ*, **865**, 59
- Yuen, K. H., Hu, Y., Lazarian, A., & Pogosyan, D. 2019, arXiv:1904.03173
- Yuen, K. H. & Lazarian, A., 2020, *ApJ*, **898**, 65
- Yuen, K. H., & Lazarian, A. 2020, arXiv e-prints, arXiv:2002.01926
- Yuen, K. H., Ho, K. W. & Lazarian, A., 2021, *ApJ*
- Yuen, K. H., Ho, K. W., Law, C. Y., Chen, A. & Lazarian, A., 2021, submitted

This paper has been typeset from a $\text{\TeX}/\text{\LaTeX}$ file prepared by the author.

APPENDIX A: TURBULENT LINE WIDTH FOR THREE PHASE MEDIUM IN NUMERICAL SIMULATION

At §3, we discussed the turbulent contribution to the line-width of *Cattail*. While the temperature of HI gas varies for two orders of magnitude in multiphase medium, its velocity distribution keeps constant throughout the phase transition. This can be shown using the multi-phase MHD simulation that we used in Yuen et al. (2021a) and Ho et al. (2021a). Fig. A1 shows the velocity distribution of three phases using the "weak field" simulation in Yuen et al. (2021a) and Ho et al. (2021a). One can see that the three phases share a highly similar distribution with approximately the same FWHM, suggesting that we can use the same turbulent line width for all phases in our analysis (§4).

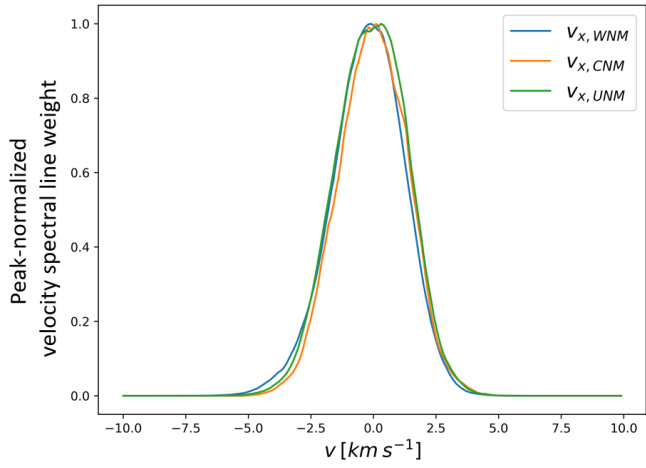


Figure A1. The velocity spectral lines for three phases in multi-phase simulation we employed in (Yuen et al. 2021a; Ho et al. 2021a), where the x-axis shows the velocity range in the unit of $km s^{-1}$ and the y-axis shows the peak-normalized velocity spectral line weight ranging from 0 to 1.